Introduction of a New Optimized Total Cavopulmonary Connection

Dennis D. Soerensen, MS, Kerem Pekkan, PhD, Diane de Zélicourt, MS,
Shiva Sharma, MD, Kirk Kanter, MD, Mark Fogel, MD, and Ajit P. Yoganathan, PhD

Wallace H. Coulter Department of Biomedical Engineering, Georgia Institute of Technology and Emory University, Atlanta, Georgia; Carnegie Mellon University, Pittsburgh, Pennsylvania; Pediatric Cardiology Associates, Department of Surgery, Emory University, Atlanta, Georgia; and Division of Cardiology, The Children's Hospital of Philadelphia, Philadelphia, Pennsylvania

Background. **Several variations of the total cavopulmonary connection (TCPC) have been investigated for favorable fluid mechanics and flow distribution. This study presents a hemodynamically optimized TCPC configuration code-named "OptiFlo." Featuring bifurcated vena cava (superior venacava to inferior vena cava SVC/IVC), it was designed to lower the fluid mechanical power losses in the connection and to ensure proper hepatic blood perfusion to both lungs.**

Methods. **A rapid prototype model of the OptiFlo TCPC was built and in vitro control volume flow analysis was performed to evaluate the fluid mechanical power loss performance of the model. Furthermore, computational fluid dynamics simulations were used to investigate the flow patterns in the model, which were compared with those in the planar one-diameter offset TCPC with flared anastomosis sites, the best known TCPC configuration to date.**

Results. **Compared with the one-diameter offset reference model, the OptiFlo showed lower power losses: −26%, −31%, and −42% for increasing cardiac outputs of 2, 4, and 6 L/minute, respectively. No statistically significant differences were found in power loss between 40:60 and 50:50 SVC/IVC flow ratios ($p > 0.1$) for the OptiFlo model. The power loss characteristic curve for different left and right pulmonary artery ratios was flatter for the OptiFlo than the one-diameter offset reference model. Pulmonary artery flow was much more streamlined in the OptiFlo compared with the one-diameter offset model.**

Conclusions. **The OptiFlo TCPC design exhibits lower power losses with better adaptive distribution of hepatic blood to both lungs and lower blood flow disturbances compared with the planar one-diameter offset TCPC model. Its significantly superior hemodynamic performance at higher cardiac outputs (exercise) rationalizes further design and feasibility studies toward a workable clinical model.**

(Ann Thorac Surg 2007;83:2182–90)

Since its introduction, the Fontan procedure has been employed as the definitive palliation for a number of congenital heart defects where a serial arrangement of pulmonary and systemic circulations is necessary. The surgical outcome has improved considerably over the years with lower mortality rates; however, patients with a Fontan procedure still suffer from connection-associated problems, leading to reduced exercise tolerance as well as serious long-term complications [1, 2] potentially reducing both duration and quality of life.

Among the multiple variables determining the outcome of the Fontan procedure, it has long been hypothesized that lowering the fluid mechanical power loss caused by the "inefficient" Fontan connection geometry could reduce the workload on the single ventricle and increase exercise capacity. This hypothesis was recently confirmed by the lumped parameter modeling studies of the single-ventricle circulation [3], where the power losses were shown to have a significant impact on the cardiac output (CO) and postoperative venous compliance remodeling. Isolated clinical cases demonstrating an acute recovery with improved designs of TCPC pathways are also reported [4]. To date, a number of suggested Fontan connection configurations have been investigated spanning from the original unidirectional connection [5] to the total cavopulmonary connection (TCPC). Despite good hemodynamics and streamlined flows going to the pulmonary arteries (PAs), the unidirectional connections resulted in poor clinical outcomes mainly due to the fact that the hepatic blood was directed exclusively to one lung causing serious pulmonary arteriovenous malformations and diminished lung growth [6–8]. Furthermore, these unidirectional configurations were not adaptive to the changes in independent pulmonary circuits. The TCPC circumvents these problems by connecting both venae cavae (VCs) to both Pas, allowing the hepatic blood to mix and be distributed to both lungs. However, the head-on collision of the caval flows was shown to have a detrimental effect, increasing the amount of energy dissipation. From a theoretical point of view, the planar one-diameter offset TCPC model with flared anastomosis sites (1D offset model) [9] proved to be the best idealized TCPC design with the lowest predicted

Accepted for publication Dec 4, 2006.

Address correspondence to Dr Yoganathan, Wallace H. Coulter Department of Biomedical Engineering, Georgia Institute of Technology & Emory University, Room 2119, U.A. Whitaker Building, 313 Ferst Dr, Atlanta, GA 30332-0535; e-mail: ajit.yoganathan@bme.gatech.edu.

Published by Elsevier Inc

0003-4975/07/$32.00
doi:10.1016/j.athoracsur.2006.12.079

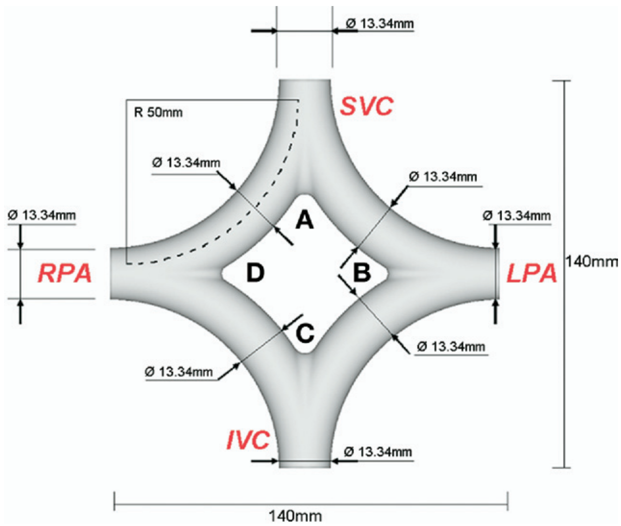

Fig 1. The new idealized total cavopulmonary connection model design, code-named OptiFlo. (IVC = inferior vena cava; LPA = left pulmonary artery; RPA = right pulmonary artery; SVC = superior vena cava.)

power losses. The caval offset prevented the head-on inflow collision, while a vortex located at the center of the connection helped redistribute the hepatic flow. On the other hand this central vortex is also an inherent source of energy dissipation and was observed to yield helical flow patterns in the PAs, increasing the friction losses even further. Further insight in to the pathway hemodynamics has been revealed by many earlier dedicated computational flow studies [10–13]. Based on these observations, this study presents an optimized Fontan connection, code-named "Optiflo," which avoids the dissipative inflow collision while still allowing for hepatic blood distribution and adaptation to flow ratio changes between the inlets and the outlets.

Material and Methods

OptiFlo TCPC Geometry

A type of TCPC connection was developed to minimize the hydrodynamic power losses and improve TCPC hemodynamics even further. The basic OptiFlo geometry is depicted in Figure 1.

Many variations of this concept are possible but this study will focus on the standard configuration with constant branch diameters, equal to the inlet and outlet diameters. To evaluate its performance relative to the previous idealized model studies [9, 14], a planar OptiFlo model was created with the same overall size, geometric characteristics, and vessel diameters of the previous idealized models. Geometric compatibility with the previous traditional TCPC models required tubular splits curved with a 50-mm radius of curvature and diameters of 13.34 mm. The splits at the VCs (A and C in Fig 1) and PAs (B and D in Fig 1) were flared with radius of curvatures of 3 mm and 2 mm, respectively.

An experimental physical model was created using the rapid prototyping technique previously described by our group [15]. The computer-aided design model was converted to a stereolithographic (STL) file and imported into, and manufactured by, a rapid prototyping (RP) machine (SLA 250; 3D Systems, Valencia, CA). A clear resin was used (RenShape SL 5510/7510; Huntsman, East Lansing, MI). To enable sanding and polishing of the inside of the model, it was created of four subparts that were later assembled together using regular cyanoacrylate adhesive.

In Vitro Hydrodynamic Power Loss Analysis

The OptiFlo configuration was investigated by a control volume flow analysis to evaluate its fluid mechanical power loss performance compared with existing idealized TCPC models. Furthermore, computational fluid dynamics (CFD) was used to elucidate the flow and velocity patterns of the connection. All experiments and CFD simulations were run under steady flow conditions.

The physical model was investigated with control volume flow analysis using an in vitro flow loop that has been described previously [9, 14]. Static pressure and flow rate measurements at each inlet and outlet were used to calculate the power loss in the model volume. The inflow conditions were steady and maintained by a constant pressure head, where the model was lying flat on a table, mimicking a supine position. Fully developed inflow profiles were achieved and a blood analogue solution of water and glycerin was used to match the viscosity of blood. Differential static pressures were measured at the wall of each vessel 2 cm away from the inlet and outlet ends. Energy losses were then computed by an integrated control volume energy balance:

$$\dot{E}_{loss} = \sum_{inlet} P_{itotal}.Q_i - \sum_{outlet} P_{itotal}.Q_i,$$

where $P_{i\ total}$ and Q_i are the total pressure and the flow rate, respectively, at an inlet (inferior vena cava [IVC],

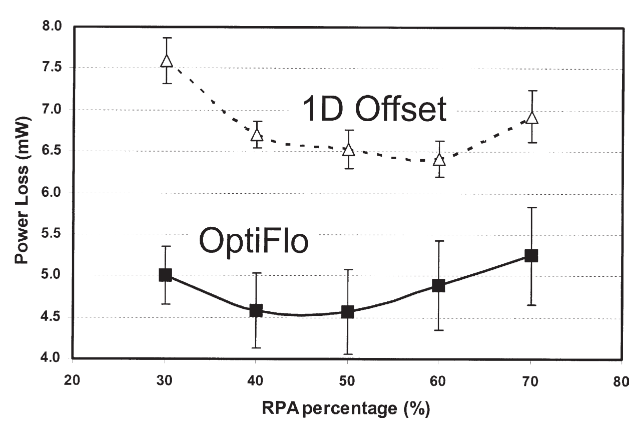

Fig 2. Power loss comparisons between the OptiFlo model (■) and flared planar one-diameter (1D) offset model (◇) at cardiac output of 4 L/minute, and with a 40:60 superior vena cava to inferior vena cava flow ratio. Both are rapid prototyping models with a 13.34-mm diameter. Error bars indicate one standard deviation. (RPA = right pulmonary artery.)

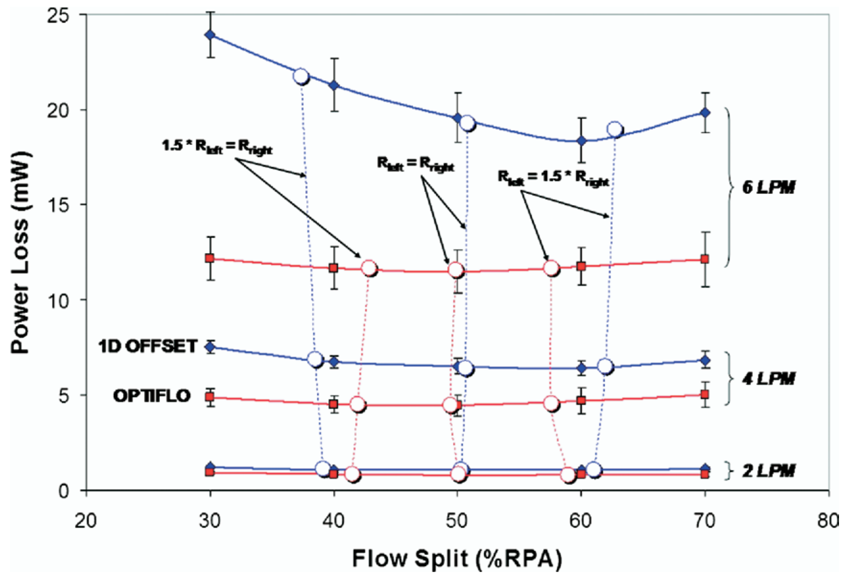

Fig 3. Power loss versus right lung perfusion (%RPA [right pulmonary artery]) at increasing cardiac outputs (2, 4, and 6 L/minute [LPM]) for the OptiFlo (red squares) and one-diameter (1D) offset reference model (blue diamonds) at a 40:60 superior vena cava to inferior vena cava flow ratio. The physiological operating points for representative left and right lung resistances (R_{left} and R_{right}) are shown with circles for both models at the three cardiac outputs (R_{right}=1.8 Woods Units).

superior vena cava [SVC]) or an outlet (left pulmonary artery [LPA], right pulmonary artery [RPA]). Power losses calculated this way for the different models were compared using a paired Student *t* test.

Flow Conditions

The total CO was chosen to be 2, 4, and 6 liters per minute (LPM). The SVC/IVC flow ratios were chosen to be 40:60 and 50:50, whereas the LPA/RPA flow ratios ranged from 30:70 to 70:30 in 10% increments. These flow values matched those of the other in vitro studies [9, 14, 16] and enabled one-to-one performance comparison with the previous idealized TCPC geometries.

Numerical Studies

To understand the detailed three-dimensional flow fields, CFD studies are performed for the OptiFlo TCPC configuration. OptiFlo geometry is created in ProEngineer (PTC Inc, TX). The overall size and the uniform vessel diameter of 13.34 mm is chosen to enable performance comparison between the planar 1D offset configuration with flared anastomosis sites representing the standard lowest power loss TCPC configuration. The CFD methodology and the computational results of the idealized 1D offset configuration have been described earlier [17, 18]. The same CFD methodology is used for the new OptiFlo configuration. Particular emphasis is given to achieve the same mesh density (finest mesh density) in both models. Computational mesh is further refined around the confluence and bifurcation regions. An unstructured mesh of approximately 98,000 nodes was generated (Gambit; Fluent Inc, Lebanon, NH) from the same STL file used for manufacturing the physical RP model. To ensure steady laminar flow at the inlet and convergence at the outlets, the inlets and outlets were extended 5 cm and 10 cm, respectively, giving 15-cm and 20-cm long inlets and outlets, respectively, when measured from the center of the model. The flow conditions were the same for the two models: steady flow with CO of 4 LPM, 40:60 SVC/ IVC ratio, and 40:60 LPA/RPA flow ratio. For both models, steady-state flow fields were computed using the parallelized segregated finite-element CFD solver FIDAP (Fluent Inc). The pressure projection algorithm with the second-order streamwise upwinding was utilized. Fourth-order convergence for the Euclidean norm of velocity and pressure was established in the presented results. This solution methodology has demonstrated good agreement with the in vitro

Table 1. Sample Average Pressure Drop Values Measured in In Vitro Experiments for the OptiFlo Configuration With Respect to the IVC Branch

Cardiac Output (L/minute)	Average Pressure (mm Hg)		
	SVC	RPA	LPA
2	−0.055	−0.200	−0.190
4	−0.256	−0.581	−0.490
6	−0.612	−0.969	−0.930

IVC = inferior vena cava; LPA = left pulmonary artery; RPA = right pulmonary artery; SVC = superior vena cava.

Table 2. Percent (%) Differences in Power Loss Between the One-Diameter Offset and the OptiFlo Models at Representative Right and Left Lung Resistance Combinations[a]

Cardiac Output (L/min)	$1.5 \times R_{left} = R_{right}$	$R_{left} = R_{right}$	$R_{left} = 1.5 \times R_{right}$
2	−24	−23	−25
4	−35	−31	−30
6	−46	−40	−38

[a] These physiological operating points are shown as circles in Figure 3 on the power loss versus pulmonary flow split performance curve.

experiments in our previous studies with more complex anatomical models [18, 19].

The Tecplot (Tecplot Inc, Bellevue, WA) software package with the CFD analyzer add-on was used for analysis of the OptiFlo models flow and velocity patterns. Power losses were determined for each of the finite elements in the CFD mesh using the viscous dissipation method as described by Healy and colleagues [20]. This method calculates power losses entirely based on the velocity gradients between the finite elements, which enables a good qualitative look at the power loss "hot spots" in the investigated volume. The higher the velocity gradient between neighboring finite element volumes is, the higher the power loss is.

Results

Hydrodynamic Power Loss

Variation of the hydrodynamic power loss for a range of LPA/RPA flow ratios were measured both for the OptiFlo configuration and for the standard 1D offset reference model [14]. Compared with the 1D offset model the OptiFlo exhibited lower power losses: $-26 \pm 4\%$, $-31 \pm 4\%$, and $-42 \pm 5\%$ for increasing cardiac outputs of 2, 4, and 6 LPM, respectively ($p < 0.01$). Figure 2 displays this difference measured for the CO of 4 LPM, with a 40:60 SVC/IVC flow ratio. For increasing CO, power loss is increased for both models (Fig 3) while the hydrodynamic advantage of Optiflo over the 1D offset model is amplified with increasing CO. The IVC/ SVC flow ratio of 50:50 did not show statistical significant effect ($p > 0.1$) in power losses compared with the 40:60 SVC/IVC flow ratios. Furthermore, the power loss curve of the OptiFlo model is found to be slightly flatter compared with the 1D offset model characteristic. Calculating the ratio between the highest power loss in these curves to that of the lowest of the same curve, the ratio for the 1D offset model is 1.19, and for the OptiFlo model the ratio is 1.15. Average branch flow rate and pressure values (with

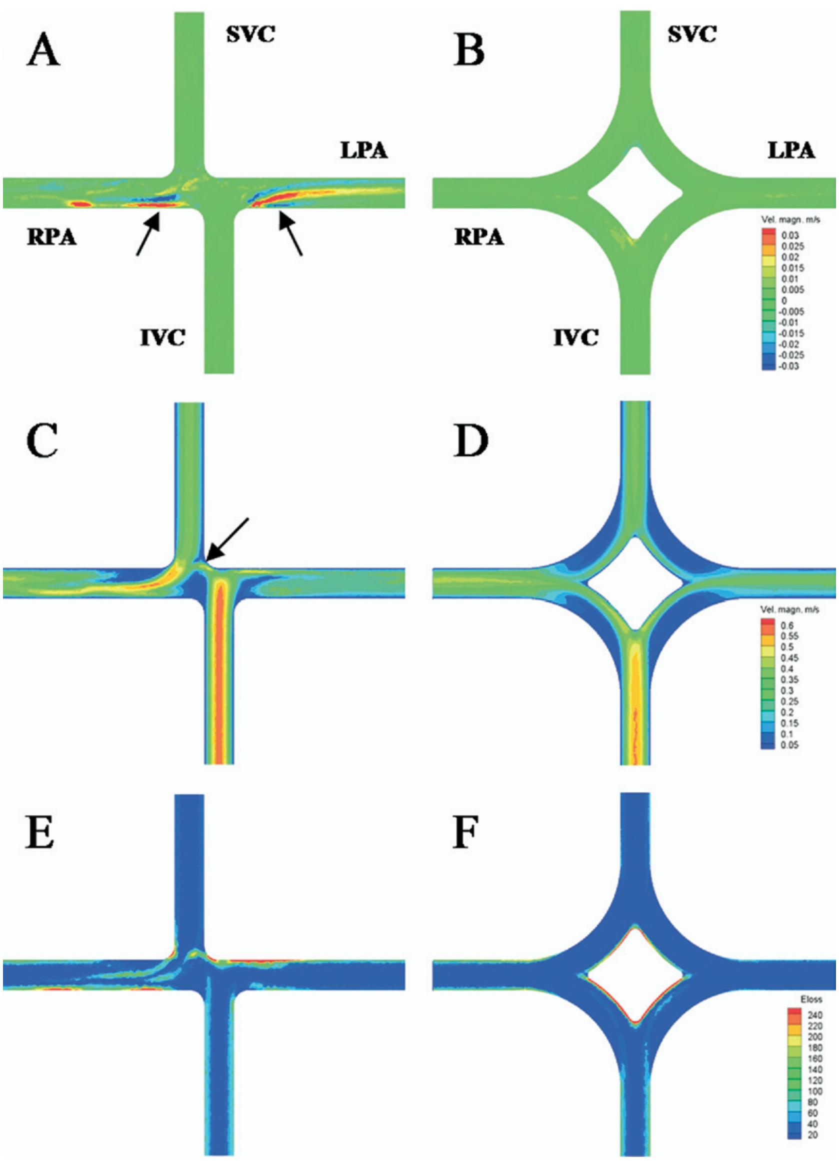

Fig 4. Flow through OptiFlo (right column) is compared with the one-diameter offset (left column) total cavopulmonary connection reference model using computational fluid dynamics simulations at a cardiac output of 4 L/minute 40:60 SVC/IVC flow ratio, and 40:60 LPA/RPA flow ratio. Three flow parameters are plotted along the midcoronal plane (that sliced both models along the coronal direction in half). (Top row, A and B) Through-plane velocity component; blue and red color tones represent flow going in and out of the page, respectively. (Middle row, C and D) Total velocity magnitudes, and (bottom row, E and F) viscous power dissipation (loss). The color coding is the same for each figure pair; A/B, C/D, and E/F, where blue color tones correspond to lower flow parameter values. Note the increasingly disturbed flow patterns and power loss hot spots of the one-diameter offset model compared with the OptiFlo. Arrows in panel A highlight the irregular pulmonary artery branch flows specific to the one-diameter offset model. Arrow in panel C indicates point of IVC stream collision. (Refer chapter on Three-Dimensional Flow Structures in text.) (IVC = inferior vena cava; LPA = left pulmonary artery; RPA = right pulmonary artery; SVC = superior vena cava.)

Ann Thorac Surg
2007;83:2182–90

respect to IVC) that are measured during in vitro experiments are summarized in Table 1 for 50:50 RPA/LPA flow ratio.

Physiological Operating Points

The computational or experimental acquisition of power loss performance at all possible pulmonary conditions further enables the calculation of the actual physiological operating point for the given left and right lung resistances. This methodology is described earlier in detail [14, 17, 19]. Following the same methodology, representative physiological operating points,including the unbalanced left and right lung resistance conditions, are calculated for both models and shown on the corresponding power loss characteristic curve (Fig 3). These revealed that the OptiFlo model favors an equal flow split (50:50 LPA/RPA) and low power loss condition even with unbalanced lung resistances. In contrast the 1D offset model tends to operate at extreme flow splits leading to higher power losses for unbalanced lung resistances. Due to this fact, at these physiological operating points power loss differences between the two TCPC configurations are slightly higher, Table 2.

Three-Dimensional Flow Structures

The 1D offset model exhibited helical flow patterns in both PAs, which are well-depicted in Figure 4A, where along the midcoronal plane of the TCPC the anterior-posterior velocity component is plotted. Higher values of this velocity component correspond to rotational flows due to the out-of-plane movement (in the anterior [shown in red color] or posterior direction [blue color]) of blood from the midcoronal plane. In contrast, the PA flow of the OptiFlo model is considerably unidirectional (Fig 4B). Minor out-of-plane blood movements from the mid-coronal plane were observed in the OptiFlo model, which is located at the flaring point (C in Fig 1) of the IVC and at the confluence site of the RPA where the splits had merged. It was observed with streamtraces (not shown here) that the flow entering the OptiFlo connection close to the anterior and posterior walls would, after the flared splitting point (marked A and C in Figure 1), cause recirculation and secondary flows. These regions correspond to the low flow regions of Figure 4D that are shown in blue color.

For both models the inlet flow profile remained fully developed upon entering the vena cava bifurcation sites (parabolic velocity variation in Figs 4C; 4D). For the OptiFlo, due to the inertia of the caval flow entering the bifurcation, the majority of the flow could not follow the outer curved wall of the model and did not split to left and right lungs until it is constrained by the inner curved wall at the splitting tip (marked A and C in Fig 1). This caused large low flow regions and flow separation in the splits contributing to the power loss. However, after the splits merged forming the PAs a laminar parabolic velocity profile was quickly established, although slightly skewed towards the superior sides of the PAs initially due to the larger share of the flow coming from the IVC.

The 1D offset model showed more disturbed flow compared with that of the OptiFlo, which is clear in both Figures 4A and 4C. One of the reasons for this was that the majority of the flow entered from the IVC and exited through the RPA. Therefore, some of the fluid entering from the IVC was forced to exit through the RPA, causing some collision of the SVC and IVC flows marked with the black arrow in Figure 4C.

The cross-sectional area of each split in the OptiFlo was equal to that of the inlets and outlets. Consequently, the velocity magnitude of the flow after the bifurcation was lower than upon entering the VCs. Furthermore, in the IVC, there was a region before the point where the flow collided with the flaring site (marked C in Fig 1), at which the velocity magnitude decreased. After the split was complete and the flow had passed the flaring site, the velocity magnitude increased again. The low velocity magnitude region was caused by the elevated pressure at the flaring site.

Local Contribution to the Power Loss

Depicting the viscous power dissipation on a color scale throughout the model provides a good insight to the flow structures causing elevated power losses which can be termed as "hot spots." From Figures 4E and 4F it was evident that there were distinct regions in both models with elevated power losses. In the OptiFlo this was observed at the inner sides of the splits where the flow collided with the splits, thus increasing the shear stresses. The flow separations between the low and high velocity flow in the splits of the OptiFlo model also increased the power losses.

The regions with elevated power losses for the 1D offset model were not as confined as for the OptiFlo model. For the 1D offset model, increased power losses were observed in four regions: (1) where the IVC flow entered the middle of the 1D offset connection colliding with the flow from the SVC (black arrow in Fig 4C): (2) the flow separation between the high velocity VC flow entering the connection and the low velocity flow in the middle of the connection; (3) the helical flow in the Pas; and (4) the walls due to wall friction and (or) flow collision. The regions with elevated power losses in the OptiFlo model were overall smaller both in size and magnitude compared with those in the 1D offset model.

Comment

Hydrodynamic Performance

In this study, the power loss characteristics of the OptiFlo configuration were compared with the 1D offset model which is known in the literature as the best performing idealized model resulting in the lowest possible power loss among the other traditional "+" shaped configurations. Achieving lower power losses than the already superior 1D offset model was a significant engineering challenge but has been possible with the OptiFlo configuration as presented in this paper.

Comparing two TCPC designs side-by-side has contributed to our understanding of the Fontan circulation and emphasized that there is still room for further hemodynamic optimization to avoid unnecessary power loss and hopefully increase the longevity of the Fontan circulation. Superior performance of the 1D offset model is usually attributed to the beneficial recirculating vortex at the center[21]. In reality, ranging the caval offset from zero to larger offset diameters reduces the shear zone (and in parallel the power loss) but does not completely eliminate it. Furthermore, "+" shaped junctions introduce complex constraints to the development of the secondary PA flows contributing the global power loss. Optiflo configuration eliminates this shear zone completely and gives more room for the secondary flows (due to VC to PA turning) to develop, which reduces the velocity gradients significantly; improving hemodynamics even further.

Having a flatter power loss curve, the OptiFlo is more tolerant to changes in flow ratios between the inlets and (or) outlets compared with traditional TCPC configurations. This is important considering that the LPA/RPA flow ratio is rarely constant and may change due to stenoses, unbalanced lung resistances, and (or) cardiopulmonary interactions. More importantly, the IVC and SVC flow contribution to the total venous return changes with respect to age[22]. In view of this fact, Fogel and colleagues [23] suggested guiding the IVC blood mainly to the larger lung through the RPA, and the SVC blood mainly to the LPA and the smaller lung when performing the Fontan operation. The design of the OptiFlo ensures proper adaptive distribution of both incoming and outgoing flow to the lungs, at no expense of increased power loss.

Equal left and right lung hepatic flow distribution (essential for normal lung development) is compromised for better power loss in the traditional "+" shaped TCPC configurations. Increasing the offset will lower the power losses; however, it will also disturb the proper distribution of the hepatic blood. It is well-recognized that the "beneficial vortex" of the 1D offset model preferentially diverts the IVC blood to the RPA if the IVC offset is toward the right lung. The new symmetric OptiFlo design naturally assures equal hepatic blood split which can be further customized by varying the split sizes to incorporate unequal left and right lung resistances.

While the OptiFlo model geometry is symmetric, there was a slight asymmetry in the experimental in vitro power loss curves (Fig 2) around the 50:50 LPA/RPA flow ratio. This is attributed to the four-part assembly of the physical OptiFlo model and to the unavoidable little grooves and bulges at the assembly lines, surface roughness, and uneven model polishing.

Results of this study are based on in vitro experimental measurements performed on the bench-top flow loops. Therefore, within the bounds of practical experimentation it could not mimic all details of the complex in vivo univentricular hemodynamics and physiology (like cardiopulmonary interactions, compliant vessels, etc) completely. At the same time, the average steady flow conditions presented in this study are considered an acceptable point for performance comparison, because the impact of the neglected components and influencing factors will be in the same order for both the traditional TCPC configuration and the proposed fluid dynamically efficient OptiFlo configuration.

Exercise Performance

Fontan patients are known to have a decreased exercise capacity as compared with healthy controls and this may have a significant impact on their quality of life, particularly as they get older. At the CFD simulated exercise conditions TCPC power loss increases in a dramatically nonlinear fashion with increasing cardiac output. On average, there is a ninefold (6 to 12) increase from baseline to the 2x-exercise and 33-fold (29 to 45) to the

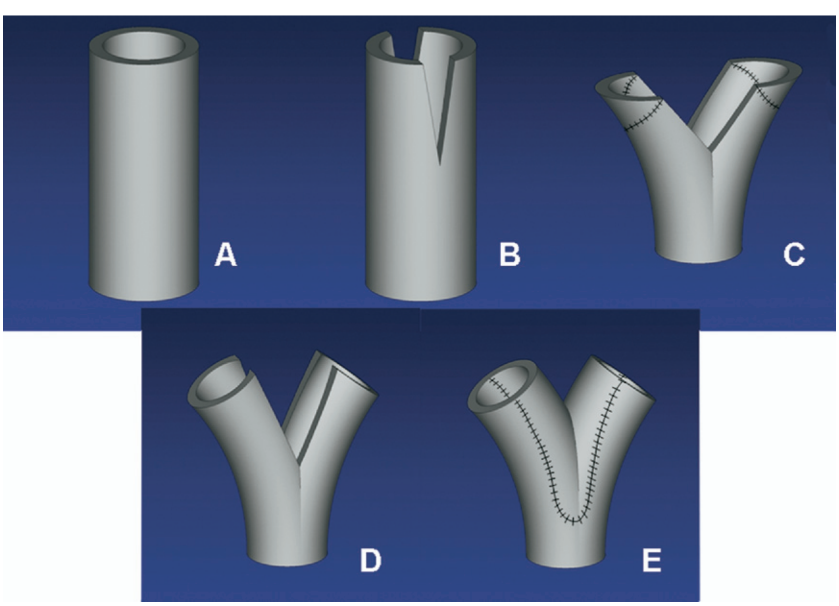

Fig 5. Five steps in the creation of split-anastomosis of the native blood vessels. (A) Vessel-end to be split-anastomosed. (B) Bisection parallel to the vessel axis. (C) Configuration for end-to-side anastomosis to branch PA, used in inferior vena cava-only split design (Fig 6B); center-piece graft not shown here. (D) Configuration for end-to-end split anastomosis (as in Fig 1); center-piece graft not shown here. (E) After the center-piece graft (Fig 6) is sutured; center-piece graft shown partially. Anticipated suture lines are shown in (C) and (E).

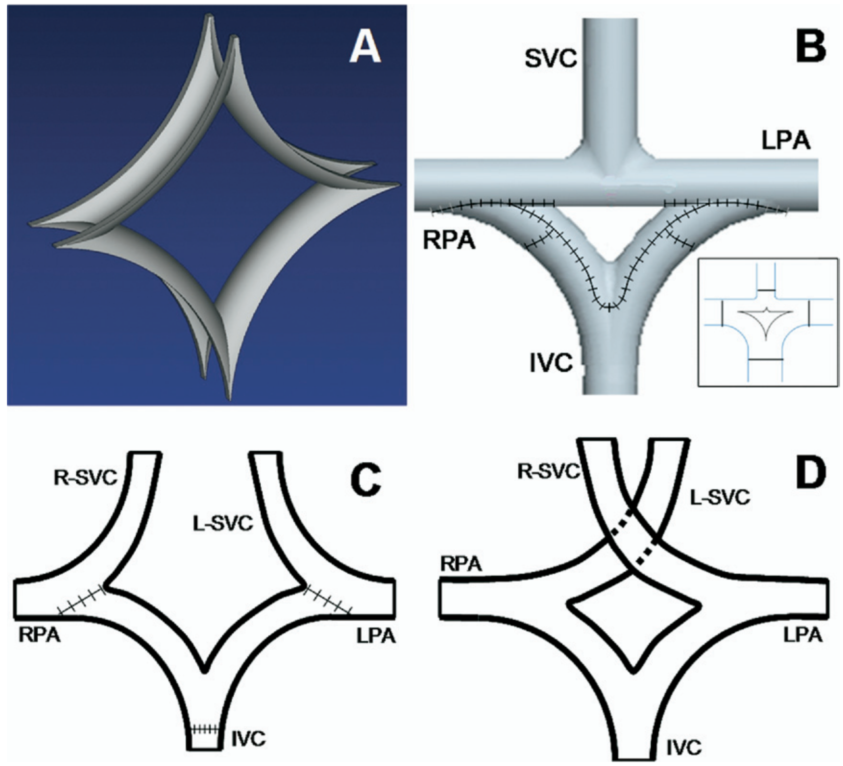

Fig 6. (A) Center-piece graft for the OptiFlo connection. (B) Alternative OptiFlo configuration with primarily IVC split. Insert illustrates an all-graft connection, where the middle part could feature a similar center-piece graft shape but now with a flatter SVC bifurcation section. (C) OptiFlo configuration for bilateral-SVC Fontan templates which utilizes a prefabricated Y-graft. (D) Alternative bilateral-SVC OptiFlo configuration with crossover SVCs. Limited feasibility, but will lead lower power loss due to increased caval-to-branch pulmonary artery pathway curvature. Anticipated suture lines are shown in (B) and (C). (IVC = inferior vena cava; L = left; LPA = left pulmonary artery; R = right; RPA = right pulmonary artery; SVC = superior vena cava.)

3x-exercise conditions in traditional anatomic TCPC connections [24]. Because the hydrodynamic benefit of OptiFlo over the traditional TCPCs increases with increasing CO, the OptiFlo configuration would be particularly advantageous at the exercise conditions. Specifically for the intense leg-exercise, only an IVC bifurcation could potentially suffice to realize the hemodynamic advantage of the OptiFlo and further eliminate a likely IVC flow recirculation into the SVC [4, 24].

Surgical Arrangement and Feasibility

The OptiFlo configuration presented here is in its most basic idealized in vitro test configuration. Its clinical utility and implementation require further more detailed considerations in order to improve its clinical feasibility through less cumbersome designs. The superior hemodynamic performance of Optiflo justifies such detailed studies, which can be undertaken in the future. In this section only some preliminary thoughts toward a workable clinical model will be presented.

The OptiFlo connection can be created using reasonably sized native vessels, as sketched in Figure 5. However, creating the connection this way would be difficult for several reasons. First, the total cross-sectional areas of the splits would only be half that of the mother vessel. Our studies showed that a reduced diameter split will act as a stenosis causing increased power losses. Second, the vessels in the TCPC are not the same size. This would cause considerable diameter mismatches between the splits from the inlets and outlets, whereby the flow in the splits would be less streamlined, increasing the power losses. Third, there might not be enough vessel material to construct the OptiFlo connection; even though the lengths of the splits would be less than the length had they been connected in a standard 1D offset configuration, the IVC ends at the right atrium level. Fourth, the shape of the splits would most likely not be curved nicely as seen in Figure 1, leading to a more rhombus-shaped connection with less streamlined PA flow mixing.

For the above reasons, a graft material is necessary for the implementation of the Optiflo TCPC in order not to compromise the superior fluid mechanical performance. Introducing graft materials will bring in growth problems but can be lessened with a partial graft as employed in intraatrial connections (Fig 6). This partial graft would then be the center part of the OptiFlo connection, where the native vessels could be connected after being bisected at the ends as illustrated in the first three steps of Figure 5.

The OptiFlo configuration could also be used in situations where blood vessels would not allow for the complete splitting and merging of VCs to the PAs. For the bilateral SVC or for small sized single SVC cases, alternative OptiFlo configurations could be useful as sketched in Figure 6. The cross-over bilateral SVC OptiFlo (Fig 6D) has the advantage over the other bilateral SVC OptiFlo (Fig 6C) option where the radius of curvature of the SVCs is larger, reducing the power losses due to the moderate secondary flow and improved streamlined PA confluence.

Future Directions

It must be emphasized again that the Optiflo geometry studied here features the most primitive and basic configuration with uniform and constant diameters. Further analysis should reveal whether the OptiFlo configuration can be improved even further. Changing the planarity, flaring of anastomosis sites, and diameters of the vessels in other idealized TCPC models have been found to affect the power losses and can be translated to the Optiflo configuration. In this study, the flaring at the bifurcation sites was found to introduce some recirculation and secondary flow. Removing the flaring at bifurcation and merging sites is likely to reduce power losses even more. Sharper bifurcations (no flaring) would avoid stagnation zones (at B and D in Fig 1) and reduce head-on wall collision (at A and C in Fig 1). For the splits, designing oval vessel cross-sections instead of the perfect circular vessel areas could control the flow separations observed at the caval bifurcations without compromising the actual flow. Changing the idealized vessel and split diameters and making them more physiologically correct will also impact the power losses in the connection. Furthermore, increasing the radius of curvature and decreasing the split length should decrease the power losses, but this speculation needs to be evaluated and quantified.

The OptiFlo configurations should be constructed using the actual surgical materials and native vessels for further in vitro flow loop tests. To evaluate its in vivo performance, the next step is to practice this configuration in an acute single ventricle animal model and, when available, in chronic experiments. These studies are essential and would reveal if the splitting and merging of venous blood return would introduce any unforeseen complications such as thrombosis and (or) stenosis formations, lung perfusion anomalies, potential kinks, or pressure build-ups.

Conclusion

A new idealized total cavopulmonary connection was introduced and evaluated with control volume flow analysis and CFD. The power loss performance of the new connection was compared with the 1D offset idealized model [9, 14, 16], which has been considered to be the best idealized model so far. The newly designed OptiFlo connection was found to exhibit lower power losses, less helical PA flow, equal distribution of hepatic blood to both lungs, and a better tolerance to varying flow splits compared with the 1D offset reference model. The new Optiflo configuration has potential to be optimized further and could be customized for use in patient-specific anatomies.

This study demonstrated that there is still room for hemodynamic improvement, up to approximately 40% in power loss, even over the "best"-known TCPC designs (1D offset configuration). While a drastically different TCPC geometry is introduced to realize this improvement to its full extent, it must be highlighted that at least some part of the presented improvement can be fulfilled in the existing traditional TCPC pathway designs with additional caution and surgical fluid flow considerations but without a drastic change in the "+" shaped TCPC configuration. By this study the traditionally "best" one-diameter offset configuration is replaced with the presented Optiflo configuration as a new target to approach for low power loss in surgical designs.

This work was supported by a BRP grant from the National Heart, Lung, and Blood Institute, HL67622. The glycerin was provided by Proctor & Gamble Co, Cincinnati, Ohio.

References

1. Gersony DR, Gersony WM. Management of the postoperative Fontan patient. Prog Pediatr Cardiol 2003;171:73–9.
2. de Leval MR. The Fontan circulation: a challenge to William Harvey? Nat Clin Pract Cardiovasc Med 2005;2:202–8.
3. Pekkan K, Frakes D, Zelicourt D, Lucas CW, Parks WJ, Yoganathan AP. Coupling pediatric ventricle assist devices to the Fontan circulation: simulations with a lumped parameter model. ASAIO J 2005;51:618–28.
4. Murakami H, Yoshimura N, Kitahara J, Otaka S, Ichida F, Misaki T. Collision of the caval flows caused early failure of the Fontan circulation. J Thorac Cardiovasc Surg 2006;132:1235–6.
5. Laks H, Ardehali A, Grant PW, et al. Modification of the Fontan procedure: superior vena cava to left pulmonary artery connection and inferior vena cava to right pulmonary artery connection with adjustable atrial septal defect. Circulation 1995;91:2943–7.
6. Srivastava D, Preminger T, Lock JE, et al. Hepatic venous blood and the development of pulmonary arteriovenous malformations in congenital heart disease. Circulation 1995; 92:1217–22.
7. Justino H, Benson LN, Freedom RM. Development of unilateral pulmonary arteriovenous malformations due to unequal distribution of hepatic venous flow. Circulation 2001; 103:E39–40.
8. Pike NA, Vricella LA, Feinstein JA, Black MD, Reitz BA. Regression of severe pulmonary arteriovenous malformations after Fontan revision and "hepatic factor" rerouting. Ann Thorac Surg 2004;78:697–9.
9. Ensley AE, Lynch P, Chatzimavroudis GP, Lucas C, Sharma S, Yoganathan AP. Toward designing the optimal total cavopulmonary connection: an in vitro study. Ann Thorac Surg 1999;68:1384–90.
10. Dubini G, Migliavacca F, Pennati G, de Leval MR, Bove EL. Ten years of modelling to achieve haemodynamic optimisation of the total cavopulmonary connection. Cardiol Young 2004;14(suppl 3):48–52.
11. Hsia TY, Migliavacca F, Pittaccio S, et al. Computational fluid dynamic study of flow optimization in realistic models of the total cavopulmonary connections. J Surg Res 2004;116:305–13.
12. Migliavacca F, Dubini G, Bove EL, de Leval MR. Computational fluid dynamics simulations in realistic 3-D geometries of the total cavopulmonary anastomosis: the influence of the inferior caval anastomosis. J Biomech Eng 2003;125:805–13.
13. Bove EL, de Leval MR, Migliavacca F, Guadagni G, Dubini G. Computational fluid dynamics in the evaluation of hemodynamic performance of cavopulmonary connections after the Norwood procedure for hypoplastic left heart syndrome. J Thorac Cardiovasc Surg 2003;126:1040–7.
14. de Zelicourt DA. A mechanical fluid assessment of anatomical models of the total cavopulmonary connection (TCPC) (MS thesis). Atlanta, GA: Georgia Institute of Technology; 2004.
15. de Zelicourt D, Pekkan K, Kitajima H, Frakes D, Yoganathan AP. Single-step stereolithography of complex anatomical models for optical flow measurements. J Biomech Eng 2005;127: 204–7.
16. Ensley AE. A fluid mechanic assessment of the total cavopulmonary connection (MS thesis). Atlanta, GA: Georgia Institute of Technology; 2000.
17. Pekkan K, Kitajima HD, de Zelicourt D, et al. Total cavopulmonary connection flow with functional left pulmonary

artery stenosis: fenestration and angioplasty in vitro. Circulation 2005;112:3264–71.
18. Pekkan K, Zelicourt D, Ge L, et al. Flow physics driven CFD modeling of complex anatomical flows-a TCPC case study. Ann Biomed Eng 2005;33:284–300.
19. de Zélicourt D, Pekkan K, Parks WJ, Kanter K, Fogel M, Yoganathan AP. Flow study of an extra-cardiac connection with persistent left superior vena cava. J Thorac Cardiovasc Surg 2006;131:785–91.
20. Healy TM, Lucas C, Yoganathan AP. Noninvasive fluid dynamic power loss assessments for total cavopulmonary connections using the viscous power dissipation function: a feasibility study. J Biomech Eng 2001;123:317–24.
21. Amodeo A, Grigioni M, Oppido G, et al. The beneficial vortex and best spatial arrangement in total extracardiac cavopulmonary connection. J Thorac Cardiovasc Surg 2002;124:471–8.
22. Salim MA, DiSessa TG, Arheart KL, Alpert BS. Contribution of superior vena caval flow to total cardiac output in children. A Doppler echocardiographic study. Circulation 1995;92:1860–5.
23. Fogel MA, Weinberg PM, Rychik J, et al. Caval contribution to flow in the branch pulmonary arteries of Fontan patients with a novel application of magnetic resonance presaturation pulse. Circulation 1999;99:1215–21.
24. Whitehead KK, Pekkan K, Kitajima H, Paridon S, Fogel M, Yoganathan A. Power loss analysis of total cavopulmonary connections under simulated exercise conditions using computational fluid dynamic analysis. The American Heart Association (AHA) Scientific Sessions, Chicago, IL, Nov 12–15, 2006.

INVITED COMMENTARY

The Fontan circulation has undergone important technical changes throughout the years. The right atrium to pulmonary artery (PA) connection has made place for the total cavopulmonary connection (TCPC), first of the lateral tunnel type and thereafter of the extracardiac conduit type. As the Fontan circulation has no right-sided ventricular driving force, all situations that cause energy loss should be avoided. The flow path must be streamlined as much as possible. Collision of caval vein flows, sharp bends, ridges, and expansions result in energy losses. A T-junction of the lateral tunnel or the extracardiac conduit and the PA is inferior in terms of energy preservation than a junction that is more curved toward one PA and thus more streamlined. In vitro models and computational fluid dynamics (CFD) studies have supported and stimulated the ongoing surgical improvements of the Fontan circulation. Several groups (Bove, de Leval and coworkers, Yoganathan and coworkers) have been working in this field for many years. They have demonstrated that an extracardiac TCPC with the inferior vena cava flow more directed toward the left PA is theoretically the optimal situation with the least loss of kinetic energy.

In the article by Soerensen and colleagues [1], further improvements of the cavopulmonary connections are presented. An innovative model of bifurcated caval veins connecting equally to both PAs is even more streamlined than the now best available technique, which is an extracardiac TCPC with offsetting of the vena cava to PA connections. The authors have demonstrated with the use of in vitro studies and CFD calculations that their prototype has lower energy losses while an even distribution of inferior caval flow to both PAs (hepatic factor) is preserved. The advantages of this model become even more evident when higher exercise conditions are mimicked by increasing the flows.

Although the bifurcated vena cava model may be superior in terms of energy preservation, the road toward clinical implication is long and full of obstacles. Will it be easy to perform this procedure in a young child? Will the risk of thrombosis be increased? What will happen with growth? These are just some of the questions that immediately arise.

However, as the theoretical advantages are evident, these obstacles should be considered as challenges for further study.

Mark Hazekamp, MD, PhD

Cardiothoracic Surgery
Leiden University Medical Center
PO Box 9600
Leiden, 2300 RC
the Netherlands
e-mail: m.g.hazekamp@lumc.nl

Reference

1. Soerensen DD, Pekkan K, de Zélicourt D, et al. Introduction of a new optimized total cavopulmonary connection. Ann Thorac Surg 2007;83:2182–90.

Published by Elsevier Inc
0003-4975/07/$32.00
doi:10.1016/j.athoracsur.2007.01.014